

# Optimal Geodesic Active Contours: Application to Heart Segmentation

Ben Appleton

Intelligent Real-Time Imaging and Sensing Group,  
School of Information Technology and Electrical Engineering  
The University of Queensland, Brisbane, Queensland 4072, Australia  
appleton@itee.uq.edu.au

## Abstract

*We develop a semiautomated segmentation method to assist in the analysis of functional pathologies of the left ventricle of the heart. The segmentation is performed using an optimal geodesic active contour with minimal structural knowledge to choose the most likely surfaces of the myocardium. The use of an optimal segmentation algorithm avoids the problems of contour leakage and false minima associated with variational active contour methods. The resulting surfaces may be analysed to obtain quantitative measures of the heart's function.*

*We have applied the proposed segmentation method to multislice MRI data. The results demonstrate the reliability and efficiency of this scheme as well as its robustness to noise and background clutter.*

## 1 Introduction

The segmentation of organs in medical images is a challenging problem due to the high geometric variation common both between subjects and within a single subject. Local feature based methods are unable to account for geometric and structural properties and often yield unreliable segmentations. Rigid templates are rarely applicable however deformable templates and active contours have more prospect for success.

Classical active contours including snakes [11] and level sets [15, 1] have shown promise in a range of medical image segmentation problems. The relatively recent geodesic active contour framework has been shown to be simple, efficient and relatively accurate [7, 9]. These methods typically use a variational framework to obtain locally minimal contours by gradient descent of an energy functional. As a result the final segmentations are dependent upon their initialisation, requiring a simpler and less reliable segmentation as input. They also have a tendency to leak through

gaps in object edges due to noise or indistinct boundaries and may become caught in irrelevant local minima.

Zhukov et. al. applied a 3D snake to segment the cavity of the left ventricle [18]. However their approach required a high level of user interaction to prevent contour leakage. To overcome the problem of contour leakage Ho et. al. used a competitive level set framework demonstrating significant improvement. They applied their approach to segment brain tumours in 3D magnetic resonance images [10].

A range of optimal active contour methods have been developed which avoid the problems of the variational framework. In the last decade numerous shortest path algorithms have been applied to locate curvilinear image features including road and valley detection from satellite images and crack detection on borehole cores [5, 6, 14].

In object segmentation the topology of the problem demands closed boundary curves. In [4] Bamford and Lovell considered the problem of segmenting nuclei in cell microscopy. They computed shortest paths across a polar trellis with the added restriction that the endpoints of the path met. The problem of shortest paths with connected endpoints was solved to optimality by Appleton and Sun [2] who used a branch and bound search to efficiently obtain the shortest closed path on trellises.

These approaches were recently unified by Appleton and Talbot to give an optimal form of geodesic active contour [3]. The resulting segmentations demonstrate superior quality to classic geodesic active contours for similar computational effort. This method is ideal for the segmentation of deformable objects characterised by homogeneous features making them attractive for medical image segmentation.

Our driving application is to assist the analysis of functional pathologies of the left ventricle in the human heart. The goal of this project is to provide quantitative measures of the heart's function, including the muscle thickness throughout the LV wall, the internal volume and the muscle volume, and the ejection fraction. Data is obtained in the form of multislice magnetic resonance images. Slices are acquired in a double oblique plane to the body along the

long axis of the heart with 10mm separation. The pixels composing each slice are  $1.4\text{mm} \times 1.4\text{mm}$ .

The aim of this paper is to present a segmentation method for this data modality which will robustly and accurately extract the epicardium and the endocardium of the left ventricle. The resulting surfaces may then be analysed to compute quantitative measures of the myocardial geometry. Due to the large separation between the slices and the lack of registration three-dimensional segmentation techniques are not considered. Instead we propose to independently segment each slice to form a layered collection of contour lines which may be suitably interpolated to approximate the myocardial surface.

## 2 Optimal Geodesic Active Contours

Our method utilises an existing algorithm for the segmentation of homogeneous objects under the geodesic active contour energy functional due to Appleton and Talbot [3]. This algorithm gives the simple closed curve of globally minimal energy which is required to contain a specified internal point  $p_{int}$ . This internal point selects the object of interest and may form the only input parameter to the algorithm, yielding a highly automated optimal object segmentation scheme.

The image to be segmented is represented as a Riemannian space  $S$  with a metric  $g$  induced by the image content. The metric quantifies the local homogeneity of the image. Using this space segmentation is achieved by locating the minimal closed geodesic containing  $p_{int}$ . A key feature of this approach is the separation of the segmentation problem into local feature extraction and global geometric optimisation.

The minimisation objective is the energy functional

$$E(C) = \int_C g(C(s)) ds \quad (1)$$

where  $C$  is the segmentation contour and  $g$  is the metric. Locally minimal contours  $C$  are known as *geodesics*. For images composed of objects characterised by homogeneous intensity we choose a positive scalar metric of the form

$$g = \frac{1}{r} \left( \frac{1}{1 + |\nabla G_\sigma \star I|^p} + \varepsilon \right) \quad (2)$$

where  $p = 1$  or  $2$  and  $r$  is the distance from  $p_{int}$ . Here  $G_\sigma$  is a Gaussian of variance  $\sigma^2$  such that the denominator is a measure of the local intensity discontinuity at scale  $\sigma$ .  $\varepsilon > 0$  is an arc-length penalty which implicitly smooths the contour. Here we alter the metric typically used in geodesic active contours [7, 9] by including an inverse radial weighting. This introduces scale invariance into the energy functional rendering it suitable for global minimisation.

Geodesics are computed on the discrete grid using Sethian's fast marching method [16, 8]. For the computation of closed geodesics we form a space  $S$  identical to the Riemann surface for the natural logarithm relation by augmenting the image plane  $\mathbb{R}^2$ . This space naturally embeds the information of whether a closed contour contains  $p_{int}$  without restricting the contour in any way.

Minimal closed geodesics are located efficiently using a best-first branch and bound search tree adapted from work by Appleton and Sun on circular shortest paths [2]. The optimal closed contour partitions the image into the object and the background such that the total similarity across the partition border is minimised.

This algorithm has been applied to the segmentation of microscope, x-ray, magnetic resonance and cDNA microarray images [3]. The resulting segmentations have been shown to be isotropic and demonstrate robustness to gaps in object boundaries as well as low sensitivity to the placement of the interior point  $p_{int}$ . They have been successfully applied to concave and convoluted boundaries, demonstrating the flexibility of this approach. The new approach compares quite favourably with the classic curve evolution approach of Caselles et. al. [7], achieving more reliable and accurate segmentations with very similar computational effort. However as opposed to classic geodesic active contours the segmentation is restricted to be a simple closed curve.

## 3 Adapting Optimal GAC

Due to the fact that the left ventricle is the major systemic pump for the cardiovascular system it has an approximately circular cross-section [13]. The internal cavity of the left ventricle appears brighter than the surrounding tissue as it is filled with blood. The myocardium appears darker than most of the surrounding tissue, with the exception of the cavity of the right lung. We therefore compute a radial gradient for each slice relative to the internal point, which is placed toward the centre of the LV. Strong negative gradients are likely to correspond to the intensity drop across the endocardium between the blood-filled LV cavity and the muscle of the myocardium, while strong positive gradients are likely to correspond to an intensity increase across the epicardium from the myocardial muscle to the generally brighter surrounding tissues.

From the radial gradient we generate a pair of metric images,  $g_{epi}$  and  $g_{endo}$ . Each metric should be low on points which are deemed likely from local features to lie on the epi- or endocardial surface respectively, and high on points which are unlikely to lie on the surface of interest. This inspires the following pair of metrics:

$$g_{epi} = \frac{1}{r} \left( \frac{1}{1 + u(\nabla G_\sigma \star I) |\nabla G_\sigma \star I|} + \varepsilon \right) \quad (3)$$

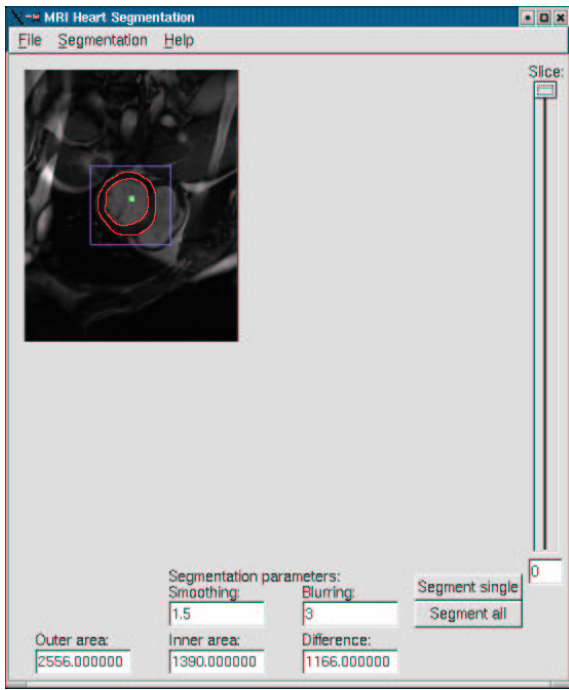


Figure 1. A snapshot of the user interface.

$$g_{endo} = \frac{1}{r} \left( \frac{1}{1 + u(-\nabla G_\sigma \star I) |\nabla G_\sigma \star I|} + \varepsilon \right) \quad (4)$$

where  $u$  is Heaviside's function [12].

Segmentation is then performed independently on each metric image using the optimal geodesic contour algorithm of Appleton and Talbot[3].

## 4 User Interface

A prototypical user interface has been designed using the FLTK cross-platform GUI builder [17] in order to develop the segmentation scheme (Figure 1). The graphical interface allows users to view each slice in turn, alter segmentation parameters such as the scale of Gaussian blurring and the contour regularity, and specify a point inside the left ventricle for the segmentation. An optional cropping box may be used to restrict the range of the segmentation contour and increase the speed of the segmentation. Segmentations may be performed on the entire dataset with common parameters or on individual slices for greater control.

## 5 Results

Figure 2 depicts a segmentation of an 8-slice dataset with common parameters. The subject was part of a research project aimed at measuring myocardial viability and had had a heart attack within the last six months. No contrast agent was used.

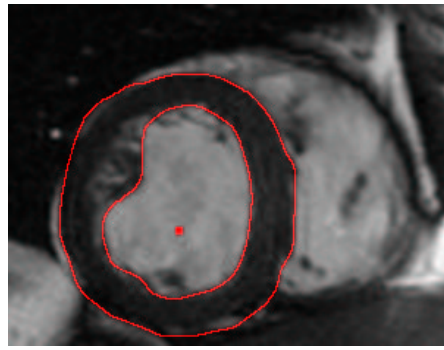


Figure 3. A single-slice segmentation at higher resolution ( $300 \times 220$ ). This slice is taken in the coronal plane and is rotated by a half circle with respect to the slices of Figure 2.

Observe that this segmentation method does not require that the slices be registered; the fifth and sixth slices are clearly misaligned by 14mm in the vertical. Despite this perturbation to the placement of  $p_{int}$  the epicardium and endocardium are still correctly segmented.

The epicardial surface is not easily distinguished by local edge strength alone due to the presence of the dark cavity in the right lung. This dark cavity produces weak edges along the heart-lung interface. Unlike classic geodesic active contours which are prone to leak through weakly defined edges the optimal geodesic active contour framework is able to correctly segment this interface in all slices.

The segmentation of the endocardial surface in the second, third and fourth slices shows a weakness of this segmentation technique. In these slices the segmentation contour follows a strong edge corresponding to a papillary muscle just interior to the superior surface of the LV cavity, instead of correctly tracking the less distinct edge of the endocardium. As a result the segmentation overestimates the thickness of the superior portion of the myocardium. This may be solved using prior structural knowledge of the heart or morphological preprocessing to remove small linear features such as papillary muscles.

All segmentations were performed on a 700MHz P-III Toshiba laptop with 192MB of RAM under the Linux operating system. The segmentation routines have been implemented in C and C++. Each slice of Figure 2 took 0.3 seconds to segment including all pre- and post-processing.

Figure 3 depicts the segmentation of a single slice at higher resolution. The increased resolution affords a better segmentation, however the computational load is greatly increased at 6.0 seconds per slice. A multiscale approach may be warranted to reduce the computational load at high resolutions.

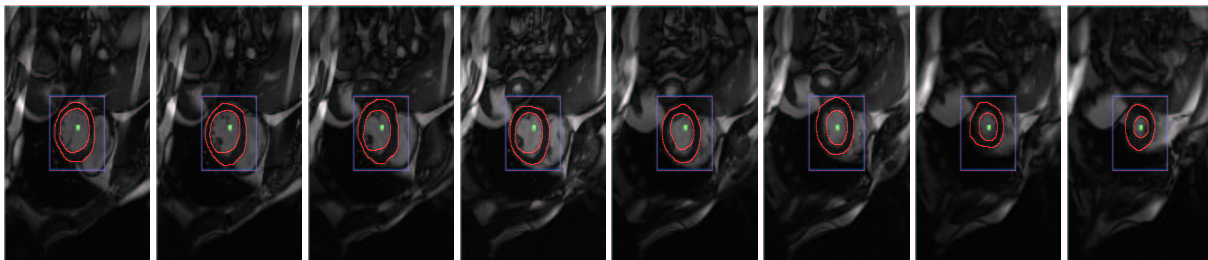


**Figure 2. A multislice segmentation of the epi- and endomyocardial surfaces of the left ventricle. Segmentation is performed within an  $80 \times 75$  crop box.**

## 6 Conclusions

We have developed an automated method to assist in the analysis of functional pathologies of the left ventricle of the human heart. To do so we propose an active contour based method for segmenting multislice heart MR data. First we compute a pair of metric images which encapsulate local knowledge about the presence of the myocardial surface. Then we apply an optimal geodesic active contour algorithm to choose the most likely closed curves in each slice corresponding to the myocardium of the left ventricle. The resulting surfaces may be analysed to compute quantitative measures of the left ventricle's function such as myocardial thickness, internal and muscle volumes and ejection fractions. In addition we designed a graphical interface to facilitate the use of this segmentation scheme and the analysis of the resulting contours (see Figure 1).

We have applied the proposed segmentation method to a multislice dataset and a higher resolution single-slice image. The results have shown that this scheme is reliable and efficient, and that it performs well in the presence of indistinct boundaries and background clutter (see Figures 2 and 3). It was shown to be confused by the inclusion of papillary muscle fibers interior to the LV, suggesting the addition of prior structural knowledge or morphological preprocessing to avoid overestimating the thickness of the myocardium in these regions.

We are currently considering ways in which an expert user may interact with the segmentation. Soft spatial weightings may be used to bias the contour optimisation toward user-specified contour points without forcing the segmentation contour to pass through an inaccurately placed point, combining the knowledge of the expert with the precision of this segmentation method.

## Acknowledgements

I would like to acknowledge Dr. Stephen Rose, Centre for Magnetic Resonance, University of Queensland and the

Centre for Advanced MRI, The Wesley Hospital, Brisbane for making available the cardiac MR data presented in this paper.

## References

- [1] D. Adalsteinsson and J. A. Sethian. A fast level set method for propagating interfaces. *Journal of Computational Physics*, 118(2):269–277, 1995.
- [2] Ben Appleton and Changming Sun. Circular shortest paths by branch and bound. *Pattern Recognition*, 2002. Submitted.
- [3] Ben Appleton and Hugues Talbot. Globally optimal geodesic active contours. *Journal of Mathematical Imaging and Vision*, 2002. Submitted.
- [4] Pascal Bamford and Brian Lovell. Unsupervised cell nucleus segmentation with active contours. *Signal Processing (Special Issue: Deformable models and techniques for image and signal processing)*, 71(2):203–213, 1988.
- [5] M. Barzohar and D. B. Cooper. Automatic finding of main roads in aerial images by using geometric-stochastic models and estimation. *IEEE Trans. Pattern Anal. Mach. Intell.*, 18(7):707–721, 1996.
- [6] M. Buckley and J. Yang. Regularised shortest-path extraction. *Pattern Recognition Letters*, 18(7):621–629, 1997.
- [7] V. Caselles, R. Kimmel, and G. Sapiro. Geodesic active contours. *IJCV*, 22(1):61–79, 1997.
- [8] Laurent D. Cohen and Ron Kimmel. Global minimum for active contour models: A minimal path approach. *International Journal of Computer Vision*, 24(1):57–78, August 1997.

- [9] R. Goldenberg, R. Kimmel, E. Rivlin, and M. Rudzsky. Fast geodesic active contours. *IEEE Trans. On Image Processing*, 10(10):1467–1475, 2001.
- [10] Sean Ho, Elizabeth Bullitt, and Guido Gerig. Level-set evolution with region competition: Automatic 3-D segmentation of brain tumors. In *Proceedings of the 16th International Conference on Pattern Recognition*, August 2002.
- [11] M. Kass, A. Witkin, and D. Terzopoulos. Snakes: Active contour models. *International Journal of Computer Vision*, 1(4):321–331, 1998.
- [12] E. Kreyszig. *Advanced Engineering Mathematics*. W. Anderson, seventh edition, 1993.
- [13] Elaine N. Marieb. *Human Anatomy and Physiology*. The Benjamin/Cummings Publishing Company, Inc., fourth edition, 1998.
- [14] N. Merlet and J. Zerubia. New prospects in line detection by dynamic programming. *IEEE Trans. Pattern Anal. Mach. Intell.*, 18(4):426–431, April 1996.
- [15] Stanley Osher and James A Sethian. Fronts propagating with curvature-dependent speed: Algorithms based on Hamilton-Jacobi formulations. *Journal of Computational Physics*, 79:12–49, 1988.
- [16] J. Sethian. A fast marching level set method for monotonically advancing fronts. In *Proceedings of the National Academy of Sciences*, volume 93(4), pages 1591–1595, 1996.
- [17] Bill Spitzak et al. The fast light toolkit home page. <http://www.fltk.org>.
- [18] L. Zhukov, Z. Bao, I. Guskov, J. Wood, and D. Breen. Dynamic deformable models for 3D MRI heart segmentation. In *Proceedings of SPIE Medical Imaging 2002*, pages 1398–1405, February 2002.